http://dx.doi.org/10.5012/bkcs.2013.34.1.211

Spectroscopic Properties of Flavonoids in Various Aqueous-Organic Solvent Mixtures

Hyoung-Ryun Park, Yu Daun,[†] Jong Keun Park,[‡] and Ki-Min Bark[‡,*]

Department of Chemistry and Research Institute of Basic Science, Chonnam National University, Gwangju 500-757, Korea
[†]Department of Chemistry and Research Institute of Life Science, Gyeongsang National University, Chinju 660-701, Korea
[‡]Department of Chemical Education and Research Institute of Life Science, Gyeongsang National University, Chinju 660-701, Korea. [*]E-mail: kiminb@gnu.ac.kr
Received September 17, 2012, Accepted November 1, 2012

The characteristic fluorescence properties of quercetin (QCT) and apigenin (API) were studied in various CH_3OH-H_2O and CH_3CN-H_2O mixed solvents. The structure of QCT is completely planar. API is not planar at the ground state but becomes nearly planar at the excited state. If the molecules are excited to the S_1 state in organic solvents, QCT exhibits no fluorescence due to excited state intramolecular proton transfer (ESIPT) between the -OH and the carbonyl oxygen, but API shows significant fluorescence because ESIPT occurs slowly. If the molecules are excited to the S_2 state, both QCT and API exhibit strong $S_2 \rightarrow S_o$ emission without any dual fluorescence. As the H_2O composition of both solvents increases, the fluorescence intensity decreases rapidly due to the intermolecular hydrogen bonding interaction. The theoretical calculation further supports these results. The change in fluorescence properties as a function of the solvatochromic parameters was also studied.

Key Words : Flavonoids, Fluorescence spectroscopy, Intramolecular charge transfer, Intramolecular proton transfer

Introduction

Flavonoids are polyphenolic compounds which are widely present in the vegetal kingdom.[1,2] Numerous investigations for the many chemical and biological activities of this family of natural substances, including antioxidant, chelating, anti-carcinogenic, bacteriostatic, and secretory activities, have been reported.[3-6] Quercetin (3,3',4',5,7-pentahydroxyflavone; QCT) is one of the most biologically active and common dietary flavonoids.[7,8] Furthermore, QCT exhibits various anomalous spectroscopic properties.[9-14] Flavonols such as QCT that contain an -OH group at position 5 (C-5) have been considered to comprise a special class of nonfluorescent molecules, and it is believed that these molecules can act as photoprotectors in that they allow the excess sunlight striking on a plant leaf to be harmlessly converted to heat.[15-18] However, when the quercetin glycoside, which also contains an -OH group at C-5, was excited to a 2nd excited state at the specific environments such as in hydro-organic mixed solvents or aerosol-OT (AOT) reverse micelle, a new significant fluorescence emission was discovered.[19,20]

To understand the mechanisms of the strong biological activities of natural compounds, it is very important to study the difference of chemical properties for two or more flavonoids with similar molecular structures. The number and position of the -OH groups in flavonoids will have a significant effect on molecule's chemical properties. Apigenin (4',5,7-trihydroxyflavone; API) is another flavonoid that exists in many plants. Compared with QCT, API also has the -OH group at C-5, but it does not have the -OH group at the C-3 and C-3' position (see Scheme 1). Other than this difference, the molecular structures of QCT and API are exactly the same. Similar to QCT, API was widely investigated due to its therapeutic potential for some diseases.[21-23] The polyphenol structure of these flavonoids makes them very sensitive to changes in their surroundings that would alter the solubility, hydrophobicity, and spectroscopic properties of these compounds and eventually lead to changes in their biological activities. Therefore, the prospect of investigating the physicochemical properties of QCT and API together in various environments, especially *in vivo*, is very attractive. However, since it is difficult to do this kind of work directly *in vivo*, many studies have been performed in biologically mimetic systems such as aqueous-organic solvent mixtures and AOT reverse micelles. The CH_3OH-H_2O and CH_3CN-H_2O mixed solvents have been considered to be especially suitable for emulating biological conditions because they show both low polarity and a partially aqueous

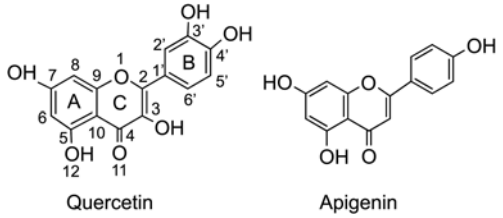

Scheme 1. The molecular structure of quercetin (3,3',4',5,7-pentahydroxyflavone) and apigenin (4',5,7-trihydroxyflavone).

Abbreviations: QCT, quercetin; API, apigenin; PMT, photomultiplier tube; ESICT, excited state intramolecular charge transfer; ESIPT, excited state intramolecular proton transfer; FC, Franck-Condon

content, always present in biological systems.[19] In this work, the comprehensive spectroscopic properties of QCT and API were studied in various CH_3OH-H_2O and CH_3CN-H_2O solvent mixtures.

Experimental

Materials. QCT and API were purchased from Sigma Chemical Co. (St. Louis, MO, USA) and used without further purification. To prevent the progressive oxidation, API was kept in the Ar gas filled container at the −20 °C. Anthracene and spectrophotometric grade CH_3OH and CH_3CN were purchased from Aldrich Chemical Co. (Milwaukee, WI, USA) and used as received. Triply distilled water was used.

Sample Preparation. Various binary mixed solvents were prepared by weight percentage. The refractive indexes of H_2O, CH_3OH, and CH_3CN are similar. In CH_3OH-H_2O and CH_3CN-H_2O solvent mixtures, the changes of π* scale (index of solvent dipolarity-polarizability) are similar to each other as the ratio of the components in the solvents is changed. The α scales (solvent hydrogen-bond donor acidity) of H_2O and CH_3OH are approximately same, but the α values of H_2O and CH_3CN are quite different. Therefore, the dielectric constants and solvatochromic parameters (π* and α) of the CH_3OH-H_2O mixed solvents are proportional to the solvent composition within the limit of experimental error. The dielectric constants, π* and α values of the CH_3CN-H_2O mixed solvents were quoted from the literatures.[19,24] It was well known that API exhibited rapid aging and oxidizing at the room temperature due to the oxygen. To avoid any opportunity to contact with oxygen, all of the stock solution and samples of API was prepared using deaerated solvents by bubbling with high purity Ar (99.999%) for about 90 min. Before fluorescence measurements, the remaining oxygen in sample solutions was removed again using Ar gas purging for 20 min. The stock solutions were also degassed by the same method and stored at −20 °C. All experiments were performed with low concentration solutions ($< 1.5 \times 10^{-5}$ M) as the samples and there were no signs of primary or secondary interfilter effects. In the preparation of QCT samples, the dissolved oxygen was also degassed using the same Ar gas purging for 20 min as described above.

Methods. The absorption spectra were obtained with a JASCO (Tokyo, Japan) V-530 UV/visible spectrophotometer. Steady-state fluorescence spectra were measured using a Perkin-Elmer (Walthan, MA, USA) LS-50B spectrofluorometer. Fluorescence quantum yields were calculated using anthracene ($\Phi = 0.27$) as a reference.[25] The fluorescence center of gravity was calculated as the position of fluorescence emission band.[20] The fluorescence lifetimes were measured using the single-photon counting method. This method was described in detail at the previously reported paper.[19]

The equilibrium structures of QCT and API were optimized with the MP2/6-31G** level using Gaussian 03.[26] The resultant structures including the molecular orbitals in three electronic states (S_o, S_1, S_2) were analyzed.

Results and Discussion

Absorption and Fluorescence Spectra. The UV-visible absorption spectra of QCT and API in various mixed solvents are shown in Figures 1 and 2, respectively. Both QCT and API contain two main absorption bands, commonly referred to as Band I (310-420 nm) and Band II (240-280 nm) for QCT, and Band I (300-390 nm) and Band II (250-280 nm) for API in both CH_3OH-H_2O and CH_3CN-H_2O mixed solvents. The peak maxima of QCT are 370 and 257 nm, while those of API are 335 and 265 nm in CH_3OH-H_2O. In CH_3CN-H_2O, the absorption peaks of QCT are 370 and 255 nm, while these bands of API are 320 and 270 nm. Compared with the absorption bands of API, Band II of QCT appears at the shorter wavelength and Band I of QCT appears at the much longer wavelength. Band I of QCT is supposed to be associated with the absorption of the cinnamoyl system (B-C ring), while Band II is associated with the absorption of the benzoyl moiety (A-C ring).[27] In CH_3OH-H_2O mixed solvents, the absorption band position of both QCT and API does not exhibit any significant changes as a function of the water composition in mixed solvents. However, the absorbance of both QCT peaks in CH_3OH-H_2O decreases gradually as the amount of water in the solvents increases. For API, the absorbance of neither peak shows any reproducible or systematic changes as a function of solvent composition in the CH_3OH-H_2O mixtures. In the CH_3CN-H_2O mixed solvents, no significant

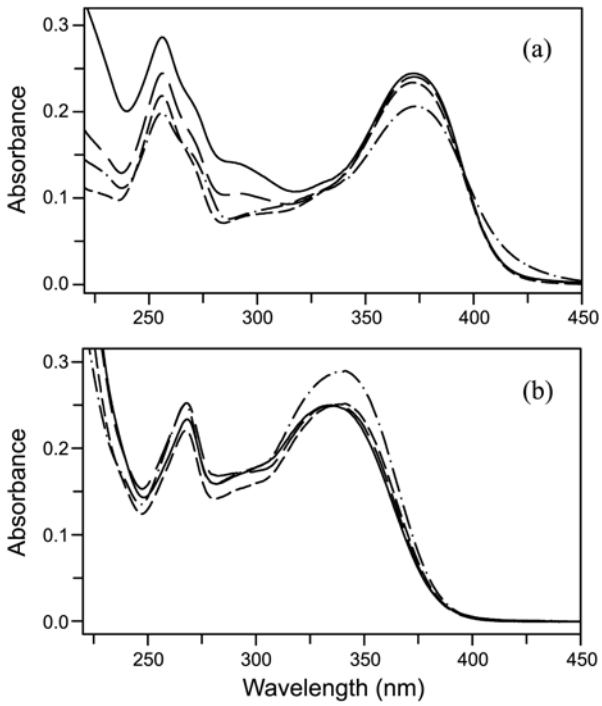

Figure 1. UV/visible absorption spectra of quercetin (a) and apigenin (b) in CH_3OH-H_2O mixed solvents. (a): (1) 100% CH_3OH (——), (2) 80% CH_3OH (– – –), (3) 60% CH_3OH (·····), (4) 40% CH_3OH (–·–·–); (b): (1) 100% CH_3OH (——), (2) 90% CH_3OH (– – –), (3) 70% CH_3OH (·····), (4) 50% CH_3OH (–·–·–).

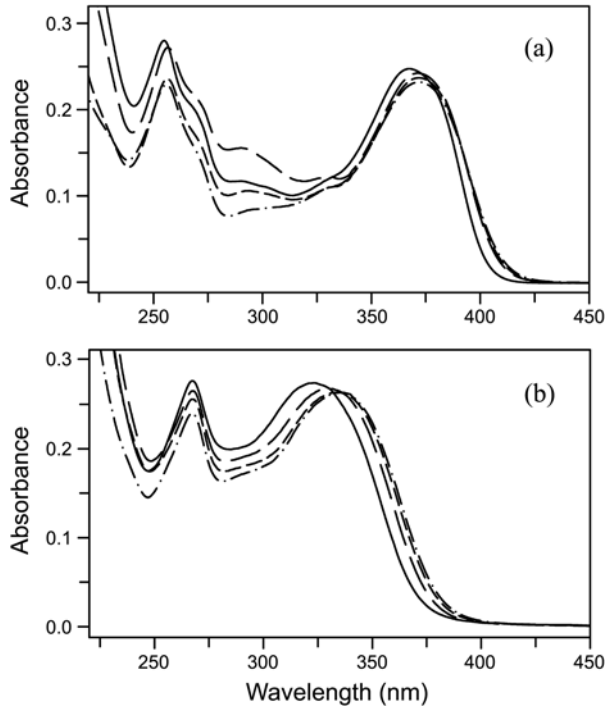

Figure 2. UV/visible absorption spectra of quercetin (a) and apigenin (b) in CH_3CN-H_2O mixed solvents. (a): (1) 100% CH_3CN (——), (2) 80% CH_3CN (– – –), (3) 60% CH_3CN (·····), (4) 40% CH_3CN (–·–·–); (b): (1) 100% CH_3CN (——), (2) 90% CH_3CN (– – –), (3) 70% CH_3CN (·····), (4) 50% CH_3CN (–·–·–).

shift of Band II is seen for either QCT or API, but a small decrease in absorbance is exhibited as the amount of water in the mixed solvent increased. However, gradual red shifts of Band I for QCT (~10 nm) and that for API (~20 nm) are shown due to the increase of water in CH_3CN-H_2O mixed solvents.

Although polyhydroxyflavones that had a 5-OH group, such as QCT and API, were regarded as nonfluorescent molecules, steady-state fluorescence emission spectra were observed for QCT and API at the various aqueous-organic mixed solvents as shown in Figures 3 and 4. As the amount of water increased in the CH_3OH-H_2O and CH_3CN-H_2O mixed solvents, the fluorescence intensity of both QCT and API gradually decreased regardless of the excitation light wavelength. When the water composition became more than about 60% for QCT and 50% for API in both the CH_3OH-H_2O and CH_3CN-H_2O mixed solvents, fluorescence emission disappeared entirely. For QCT, if 370 nm radiation (corresponding to the absorption maximum of Band I) was used as an excitation light, no fluorescence emission was exhibited in the CH_3OH-H_2O and CH_3CN-H_2O mixed solvents. However, for API, when the light corresponding to the absorption maximum of Band I (325 nm) was irradiated, strong fluorescence emission was shown in both mixed solvent systems. This phenomenon is the most critical difference between QCT and API in fluorescence properties. When the excitation light wavelength (λ_{ex}) = 255 nm (absorption maximum of Band II) was illuminated to QCT in CH_3OH-H_2O, the

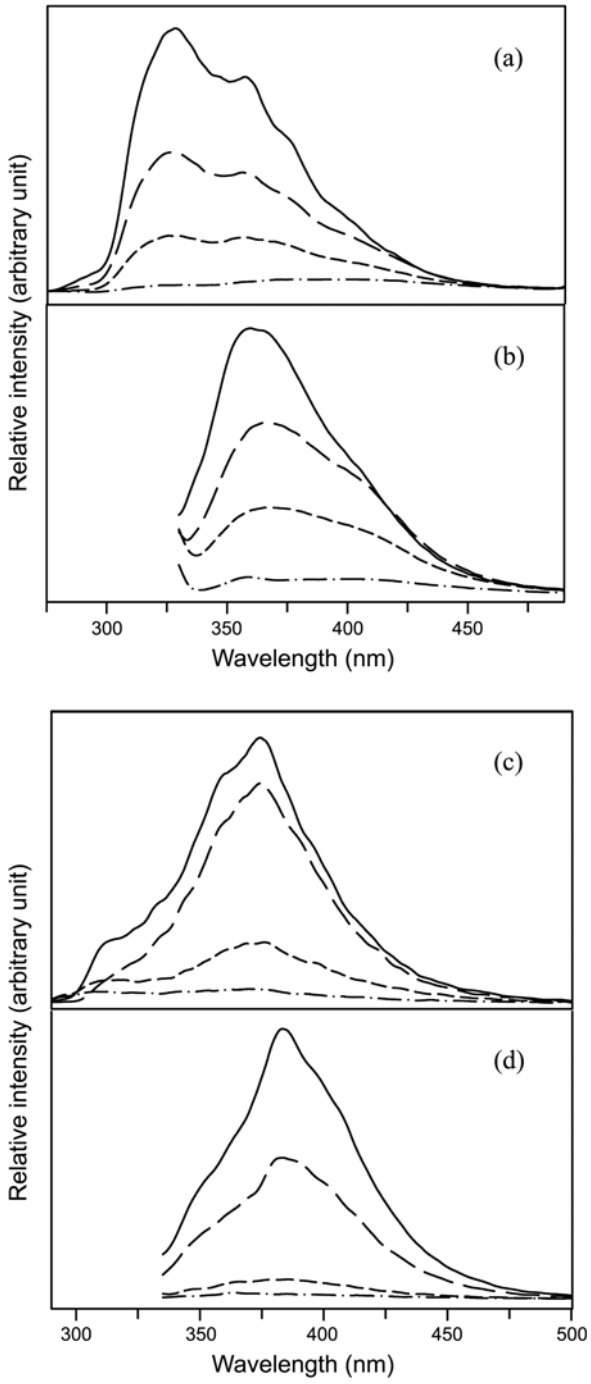

Figure 3. Steady-state fluorescence emission spectra of quercetin (QCT) (a, λ_{ex} = 255 nm; b, λ_{ex} = 320 nm) and apigenin (API) (c, λ_{ex} = 260 nm; d, λ_{ex} = 325 nm) in CH_3OH-H_2O mixed solvents. For QCT: (1) 100% CH_3OH (——), (2) 80% CH_3OH (– – –), (3) 60% CH_3OH (·····), (4) 40% CH_3OH (–·–·–); for API: (1) 100% CH_3OH (——), (2) 90% CH_3OH (– – –), (3) 70% CH_3OH (·····), (4) 50% CH_3OH (–·–·–).

strong emission maximum appeared at 330 nm but several sub-peaks also appeared at the long wavelength side of the band, ~360, ~375 nm, *etc.* as shown in Figure 3(a). At the λ_{ex} = 320 nm, peak maximum appeared at 370 nm and this band exhibited small red shift as the water composition in solvent increased (see Figure 3(b)). The fluorescence emission

spectra of API in CH_3OH-H_2O were shown in Figures 3(c) and (d). When a λ_{ex} = 260 nm light (absorption maximum of Band II) was used, the emission peak maximum appeared at 375 nm. At the short wavelength side from the peak maximum, many sub-bands were observed. When a λ_{ex} = 325 nm light (absorption maximum of Band I) was used, the peak maximum moved slightly to the long wavelength side. According to the previous study, the fluorescence emission spectra of API, which was extracted from plant and isolated using preparative HPLC, exhibited a double emission at 430 and 534 nm.[28] This extracted API should be oxidized and aged fully because that material was left in air for a long time at room temperature. It would take a lot of time for extraction from plants and isolation process. This oxidized and aged sample can exhibit different fluorescence properties without any great changes of absorption spectra. Furthermore, although the dissolved oxygen in the samples must be removed clearly to obtain correct fluorescence spectra, the samples in that work were not deaerated. So, the fluorescence intensity will decrease and the shape of spectra will change due to this dissolved oxygen. Owing to these reasons, the spectral features in Figure 3 do not coincide with the previously reported spectra. The fluorescence emission spectra of QCT and API in CH_3CN-H_2O mixed solvents were shown in Figure 4. The shapes and band position of the QCT's fluorescence emission spectra in CH_3OH-H_2O and CH_3CN-H_2O were similar. When a λ_{ex} = 325 nm light was used on API, a small red shift of the peak maximum was seen compared with the emission spectra obtained using a λ_{ex} = 260 nm light. The fluorescence emission spectra of API measured using a λ_{ex} = 260 nm light in CH_3OH-H_2O and CH_3CN-H_2O mixed solvents were somewhat different from each other. The emission peak in the CH_3CN-H_2O solvents was broad, structureless, and approximately Gaussian shape band with large Stokes' shifts. As such, for both QCT and API, the rough mirror image correlation between the absorption and emission spectra was absent in both hydro-organic mixed solvents. It is suggested that this absence of a mirror image correlation may be the result of an interaction between the emitting state and the other near excited state.[29]

To obtain further information about the fluorescence properties of QCT and API, fluorescence excitation spectra were measured in CH_3OH and CH_3CN as shown in Figure 5. Bands I and II of QCT appeared around 280 and 230 nm, respectively. Compared with the peaks of the absorption spectra (~370 and ~255 nm), Band I of the excitation spectra was greatly shifted to the short wavelength side. Band II showed a relatively small blue shift. This observation of QCT provides supporting evidence that the main absorbing species of Band I is not fluorescent.[19] For the excitation spectra of API, the blue shift of Bands I and II compared with those of absorption spectra were small in the CH_3OH and CH_3CN solvents. Band II of API in CH_3CN (~270 nm) was shifted to the long wavelength side around 15 nm compared with that in CH_3OH. Therefore, the excitation spectra of QCT and API were important evidence to explain

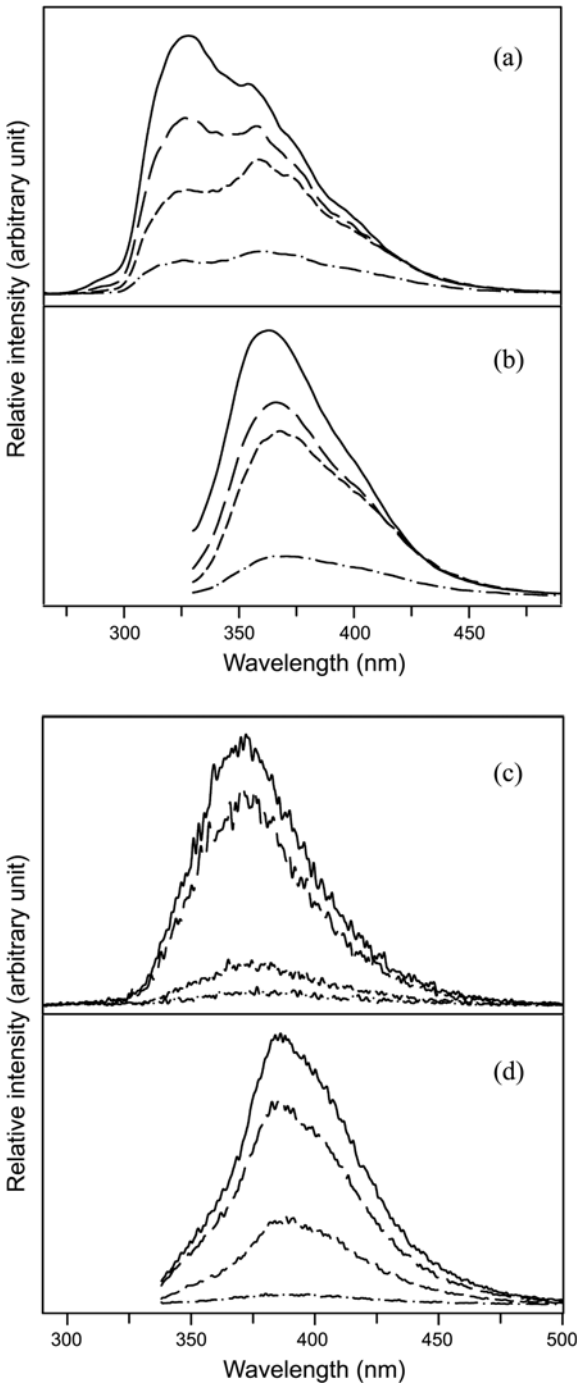

Figure 4. Steady-state fluorescence emission spectra of quercetin (QCT) (a, λ_{ex}=255 nm; b, λ_{ex}=320 nm) and apigenin (API) (c, λ_{ex}=260 nm; d, λ_{ex}=325 nm) in CH_3CN-H_2O mixed solvents. For QCT: (1) 100% CH_3CN (——), (2) 80% CH_3CN (– – –), (3) 60% CH_3CN (·····), (4) 40% CH_3CN (–·–·–); for API; (1) 100% CH_3CN (——), (2) 90% CH_3CN (– – –), (3) 70% CH_3CN (·····), (4) 50% CH_3CN (–·–·–).

the different fluorescence properties of these two molecules in hydro-organic mixed solvents. Since the fluorescence excitation spectra of API were sensitive to the change of solvent composition, the excitation spectra of API were measured at the various CH_3OH-H_2O and CH_3CN-H_2O mixed solvents as shown in Figure 6. In both mixed solvents,

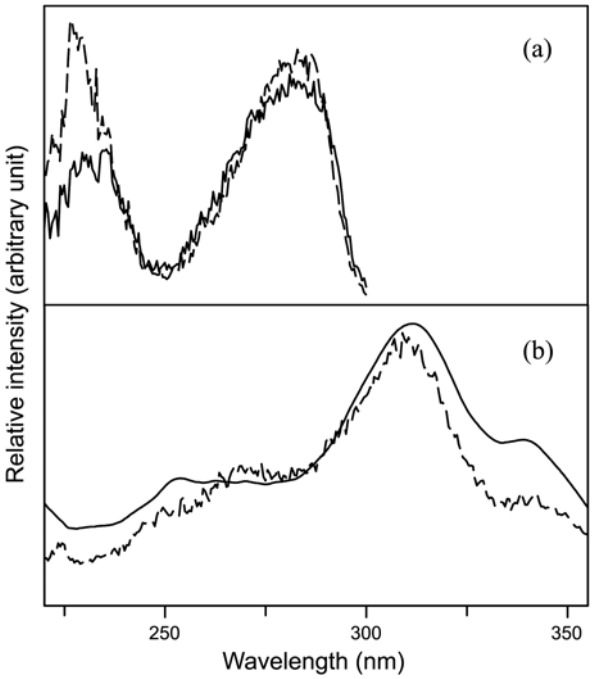

Figure 5. Steady-state fluorescence excitation spectra of quercetin (a) and apigenin (b). (a) CH_3OH (——), CH_3CN (-------); λ_{em} = 320 nm; (b) CH_3OH (——), CH_3CN (-------); λ_{em} = 370 nm.

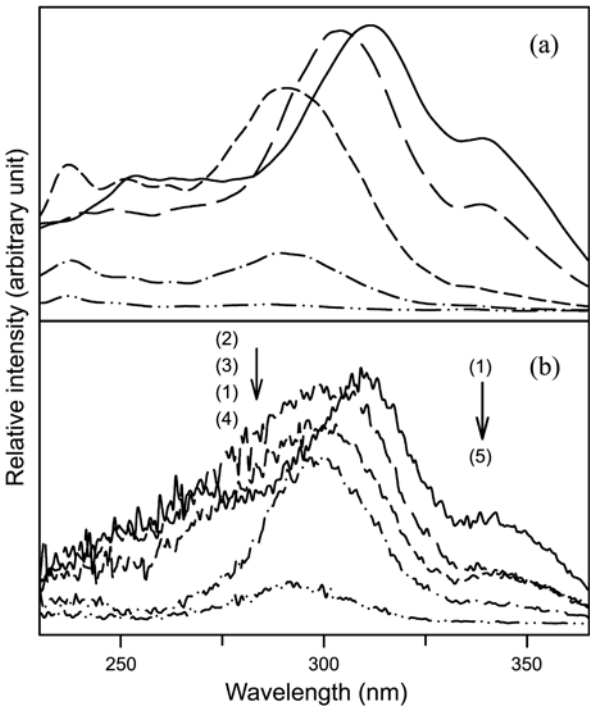

Figure 6. Steady-state fluorescence excitation spectra of apigenin in CH_3OH-H_2O (a, λ_{em}=375 nm), and CH_3CN-H_2O (b, λ_{em} = 375 nm) mixed solvents. (a): (1) 100% CH_3OH (——), (2) 90% CH_3OH (- - - - -), (3) 80% CH_3OH (-------), (4) 70% CH_3OH (-·-·-·-), (5) 50% CH_3OH (-··-··-). (b); (1) 100% CH_3CN (——), (2) 90% CH_3CN (- - - - -), (3) 80% CH_3CN (-------), (4) 70% CH_3CN (-·-·-·-), (5) 50% CH_3CN (-··-··-).

Band I exhibits a blue shift from ~310 nm to ~290 nm as the amount of water in solvent increases. This blue shift of the absorption peak is more remarkable in CH_3OH-H_2O solvents. This peak position change is consistent with the decrease of fluorescence emission intensity as the water concentration in mixed solvents increases. In CH_3CN-H_2O solvents, the small sub-band around 270 nm decreases to nearly zero as the water composition in the solvent exceeds 30%.

Molecular Geometrical Structure and the Excited State Intramolecular Charge and Proton Transfers. To understand the characteristic fluorescence properties of QCT and API, it is very important to examine the geometrical molecular structure of these compounds, especially the position of the B ring with regard to the γ-pyrone ring (A and C rings). This dihedral angle θ is determined through several effects: the repulsion caused by the steric hindrance, the various intramolecular hydrogen bonding and the effect of electronic conjugation. Since the intramolecular hydrogen bonding is known to be a more important stability criterion than steric hindrance in these molecules, the investigation of this hydrogen bonding interaction will be one of the most essential works for understanding the properties of these molecules.[19,30] QCT forms two important intramolecular hydrogen bonds between 5-OH and O-11, and 3-OH and O-11. The intramolecular hydrogen bond between 3-OH and O-11 is weaker than that between 5-OH and O-11, which forms a six-membered ring that is sterically and energetically favored.[31,32] API has one intramolecular hydrogen bond between 5-OH and O-11. The dihedral angle between the phenyl ring B and the γ-pyrone ring can change easily according to the crystalline or isolated state since the energy difference between the constrained structure and the totally relaxed structure is very small. As such, the conformational changes of QCT and API with the physical state are limited to the inter-ring link and the molecular structure can easily approach the planar.[31] It was suggested for QCT that the hydrogen bond-like interaction existed between the proton on 2' or 6' of the B ring and the 3-OH moiety. Due to this interaction, the optimized structure of QCT was completely planar in the gas phase, *i.e.*, the dihedral angle of the B ring with the γ-pyrone ring was close to 0°. Eventually, the QCT was completely conjugated. In the molecules without the 3-OH such as API, the B ring was slightly twisted relative to the plane of the A and C rings at about 17° in the S_o state; thus, the B ring was not completely conjugated to the rest of the molecule. However, in the S_1 state, API became almost planar, characterized by the dihedral angle of only 2.8°.[33-35]

Since the oxygen at the 1-position becomes an electron donor, while the keto oxygen at the 11-position serves as a good electron acceptor, QCT and API will be good donor-acceptor-conjugated molecules. As the B ring becomes coplanar with the γ-pyrone ring in the excited state, the initial molecular species will be changed to the charge transferred zwitterionic form induced by the excited state intramolecular charge transfer (ESICT).[19,20] This zwitterionic form is stabilized due to the delocalization of the π electrons throughout the molecule. In aqueous solution, the intermolecular hydrogen bond between the polar groups of the solute and the water molecules will overwhelm the intra-

molecular hydrogen bond. Since the dihedral angle θ will be relatively large in this case, it is very difficult to expect the occurrence of the ESICT.[30] Because the pseudo-Jahn-Teller distorted excited state will be formed due to the near degeneracy of the π,π* and n,π* states, radiationless deactivation processes such as internal conversion will be very fast.[15,19,29] As a result, the fluorescence emission of QCT and API will be almost totally absent in aqueous solution. However, in CH_3OH, the number of molecules having various intramolecular hydrogen bonds will be greatly increased and in CH_3CN, every solute molecule will have possible intramolecular hydrogen bonds. Therefore, ESICT should occur in organic solvents due to the effect of electronic conjugation. Again, the number of molecules forming the distorted excited state, which explains the nonradiative decay pathway, will decrease in CH_3OH, and the probability of this excited state appearing will decrease further in CH_3CN.[15,29] Since the additional resonance forms in the excited state due to the ESICT usually lead to a strong fluorescence emission, QCT and API can exhibit fluorescence spectra in the organic solvents.

Various studies about the excited state intramolecular proton transfer (ESIPT) between 3-OH and O-11 and 5-OH and O-11 by "keto-enol tautomerization" *via* intramolecular hydrogen bonding have been done for many flavonoids.[16,20,36,37] The potential energy surfaces of QCT and API in the gas phase are similar to each other.[20] The happening of ESIPT can be understood easily by considering the π electron nodal pattern of the wavefunction. These nodal planes of QCT and API are basically the same.[20] It is worth noting that ESIPT can also occur at the API from 5-OH to O-11 in the S_1 geometry, the same way as the QCT.[35] However, for both QCT and API, the S_2 state should be much less susceptible to ESIPT than the S_1 state.[20] Similarly, because the π,π* and n,π* states are close together and the nuclear frameworks are significantly different in these electronic states, internal conversion will occur rapidly.[15,19,29] Eventually, for QCT, almost all of the $S_1 \rightarrow S_o$ fluorescence emission disappears due to this ESIPT.[15,19,20] However, contrary to the case of QCT, the ESIPT of API to produce the enol tautomer at the S_1 state cannot occur quickly because the dihedral angle between the B ring and γ-pyrone ring should decrease to cause ESIPT after excitation.[35] Several theoretical studies for API suggest that upon excitation to the Franck-Condon (FC) point, the first relaxation process occurs through molecular planarization. From the FC region, the excited state energy decreases rapidly to a flat region that corresponds to the ESIPT minimum structure. The $S_1 \rightarrow S_o$ fluorescence emission of API may be due to the emission from an excited state structure that has not yet undergone the ESIPT process.[33,35] If these molecules are excited to the S_1 state, QCT does not emit any significant fluorescence, but API exhibits strong fluorescence emission in organic solvents. For QCT and API, ESICT can occur, whereas the ESIPT can not at the S_2 state in organic solvents. Due to this reason, when the QCT and API molecules are pumped to the S_2 state, strong $S_2 \rightarrow S_o$ fluorescence emission appears. Because the FC

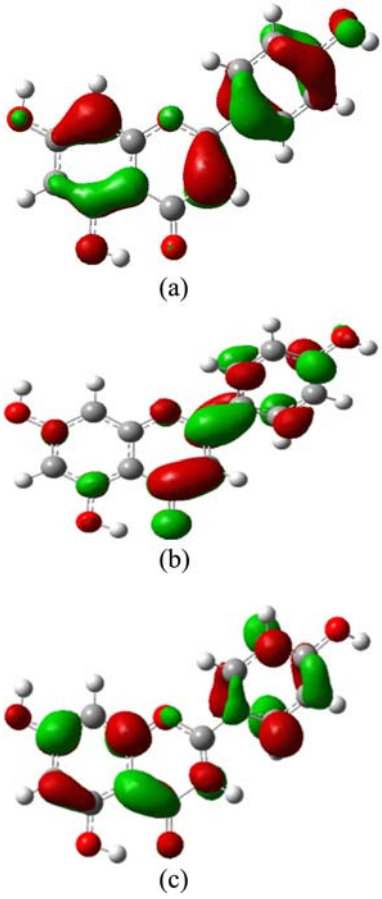

Figure 7. The optimized equilibrium structures with the molecular orbitals of apigenin (API) at the MP2/6-31G** level; (a) S_o, (b) S_1, (c) S_2.

factors involved in the $S_2 \rightarrow S_1$ radiationless transition will be very small, QCT and API do not show any dual fluorescence despite their molecules being excited to the S_2 state.[20] The optimized structure with the molecular orbital of API is shown in Figure 7 but this structure of QCT is described in the previous publication.[19] The molecular orbitals are simply described by the probability density, which emphasizes the differences in magnitude for the different atoms. At the S_o state, the phenyl linkage [C(2)-C(1')] of both QCT and API has an anti-bonding characteristic. This inter-ring bond in QCT has some π bonding characteristics due to the conjugation of π electrons, but the same bond in API has no π bonding characteristics. At the S_1 state, the [C(2)-C(1')] inter-ring bonding of both QCT and API has a bonding characteristic, and the molecular structure and the electronic charge density of these two molecules are similar. At the S_2 state, the [C(2)-C(1')] bond of QCT has some bonding characteristics, but the same bond of API has an anti-bonding characteristic. The electronic charge density of the B ring of API is larger than that of QCT. These results support the facts that at the S_o state, the molecular structure of QCT is completely planar, whereas the B ring of API deviates slightly from the γ-pyrone ring. At the S_1 state, the optimized molecular structure of both QCT and API is

Table 1. The fluorescence center of gravity (ν_f), fluorescence quantum yields (Φ), fluorescence lifetimes (τ), and radiative (k_r) and nonradiative rate constants (k_{nr}) of quercetin, and the solvatochromic parameters of the various binary mixed solvents

Solvents	ν_f (nm)[a]	Φ (10^{-3})[b]	τ (ns)[b]	k_r (10^6 s^{-1})	k_{nr} (10^8 s^{-1})	π^*[c]	α[d]
CH_3OH-H_2O[e]							
100	381	23.7	3.34	7.10	2.92	0.600	0.98
90	382	19.4	2.73	7.11	3.59	0.690	1.01
80	386	15.7	2.34	6.71	4.21	0.762	1.02
70	390	13.8	1.96	7.04	5.03	0.831	1.04
60	390	9.61	1.67	5.75	5.93	0.880	1.06
50	395	5.72	1.37	4.18	7.26	0.930	1.07
40	400	3.01	1.01	2.98	9.87	0.992	1.09
CH_3CN-H_2O[e]							
100	376	20.9	4.81	4.35	2.04	0.750	0.190
90	379	19.2	4.35	4.41	2.25	0.770	0.721[f]
80	382	16.9	3.69	4.58	2.66	0.801	0.840
70	383	16.0	3.17	5.05	3.10	0.840	0.890
60	385	14.1	2.13	6.62	4.63	0.880	0.892
50	386	9.49	1.60	5.93	6.19	0.921	0.900
40	389	6.88	1.17	5.88	8.49	0.972	0.902

λ_{ex} = 320 nm. [a]Uncertainty ≤ 1%. [b]Uncertainty ≤ 5%. [c]Index of solvent dipolarity-polarizability. [d]Solvent hydrogen-bond donor acidity. [e]Weight % of CH_3OH or CH_3CN in mixed solvents. [f]This value has relatively large uncertainty (≤ 5) because of the abrupt change with increased H_2O in mixtures

planar.

Fluorescence Property Changes as a Function of Solvent Parameters. To further study the excited state physical and chemical processes as a function of solvent properties, the fluorescence center of gravity, quantum yields, fluorescence lifetimes, and radiative (k_r), and nonradiative rate constants (k_{nr}) were calculated as shown in Tables 1, 2, and 3, and the dependence of these fluorescence properties on the π^* and α values of the mixed solvents was examined.[19] To investigate the change of fluorescence properties due to different excitation wavelengths, the fluorescence spectra were measured using λ_{ex} = 320 nm and 255 nm lights for QCT and λ_{ex} = 325 nm and 260 nm lights for API. For QCT, when λ_{ex} = 320 nm, the spectra exhibited a small red shift in the fluorescence center of gravity in the CH_3OH-H_2O (19 nm) and CH_3CN-H_2O (13 nm) mixed solvents, whereas when λ_{ex} = 255 nm, a relatively large red shift (30 nm) was shown in CH_3OH-H_2O and small red shift (13 nm) was observed in CH_3CN-H_2O as the amount of water in both mixed solvents increased. For API, when the λ_{ex} = 325 nm and 260 nm lights were used, a small blue shift (14-17 nm) in the spectra was exhibited in CH_3OH-H_2O but not in CH_3CN-H_2O due to the increase of water composition in the mixed solvents. The quantum yields of QCT and API decrease gradually regardless of excitation light wavelength in both CH_3OH-H_2O and CH_3CN-H_2O as the amount of water in solvents increases. When λ_{ex}= 320 nm for QCT and λ_{ex} = 325 nm for API, the quantum yields of API decrease more quickly than those of QCT due to the increases of water in the CH_3OH-H_2O and CH_3CN-H_2O mixed solvents. For QCT, the quantum yields measured using λ_{ex} = 255 nm are slightly smaller than those obtained using λ_{ex} = 320 nm in both mixed solvents. The quantum yield usually decreases as excitation energy increases. The decrease of quantum yields measured using λ_{ex} = 320 nm and λ_{ex} = 255 nm also exhibit similar patterns as the increase of water in the mixed solvents. For API, as the amount of water increases in both mixed solvents, the quantum yields measured using λ_{ex} = 325 nm decreases more quickly compared with those obtained using λ_{ex} = 260 nm. Also, the quantum yields of API measured using λ_{ex} = 325 nm are smaller than those obtained using λ_{ex} = 260 nm. This fact suggests that different fluorophores emit fluorescence as the API is pumped to different excited state using 325 and 260 nm radiation, respectively. This statement is further supported by the fact that the shape of emission spectra obtained using λ_{ex} = 260 nm and λ_{ex} = 325 nm is different from each other in both CH_3OH-H_2O and CH_3CN-H_2O as shown in Figures 3 and 4. As such, it

Table 2. The fluorescence center of gravity (ν_f), fluorescence quantum yields (Φ), fluorescence lifetimes (τ), and radiative (k_r) and nonradiative rate constants (k_{nr}) of apigenin in the various binary mixed solvents

Solvents	ν_f (nm)[a]	Φ (10^{-3})[b]	τ (ns)[b]	k_r (10^6 s^{-1})	k_{nr} (10^8 s^{-1})
CH_3OH-H_2O[c]					
100	395	9.78	2.67	3.66	3.71
90	395	4.51	2.13	2.12	4.67
80	394	2.28	1.52	1.50	6.56
70	387	0.756	0.94	0.80	10.63
60	382	0.370	0.53	0.70	18.86
50	381	0.190	0.14	1.36	71.41
CH_3CN-H_2O[c]					
100	395	17.7	4.00	4.43	2.46
90	396	12.9	3.58	3.60	2.76
80	397	8.98	3.23	2.78	3.07
70	397	5.82	2.78	2.09	3.58
60	397	1.68	2.33	0.72	4.28
50	397	0.739	1.79	0.41	5.58

λ_{ex} = 325 nm. [a]Uncertainty ≤ 1%. [b]Uncertainty ≤ 5%. [c]Weight % of CH_3OH or CH_3CN in mixed solvents

Table 3. The fluorescence center of gravity (ν_f) and fluorescence quantum yields (Φ) of quercetin and apigenin in the various binary mixed solvents. λ_{ex} = 255 nm for quercetin and λ_{ex} = 260 nm for apigenin

Solvents	QCT		API	
	ν_f(nm)[a]	Φ (10^{-3})[b]	ν_f(nm)[a]	Φ (10^{-3})[b]
CH_3OH-H_2O[c]				
100	351	21.3	378	14.1
90	353	19.5	377	12.0
80	356	15.6	378	10.1
70	361	12.3	371	4.97
60	363	7.94	367	2.34
50	372	3.48	361	1.03
40	381	1.96		
CH_3CN-H_2O[c]				
100	352	15.7	378	16.0
90	354	14.7	378	13.9
80	357	13.2	380	12.3
70	358	10.9	379	9.70
60	361	9.59	380	4.58
50	362	6.26	380	3.40
40	365	3.74		

[a]Uncertainty ≤ 1%. [b]Uncertainty ≤ 5%. [c]Weight % of CH_3OH or CH_3CN in mixed solvents

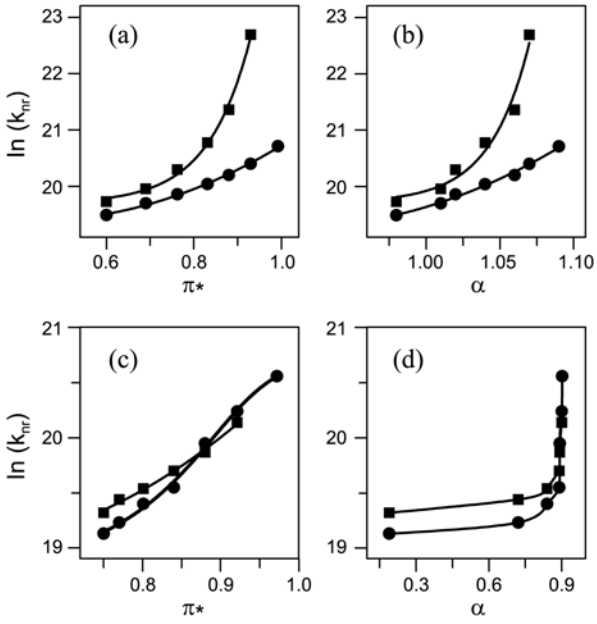

Figure 8. Logarithm of the nonradiative rate constants (k_{nr}) plotted as a function of the solvent polarity parameter (π^*) or hydrogen-bond donating strength (α) in the CH_3OH-H_2O (a, b) and CH_3CN-H_2O (c, d) solvent mixtures; quercetin (●) and apigenin (■). The solid lines are the best polynomial regression fits to the data.

can be proposed that the spectra obtained using λ_{ex} = 260 nm correspond to $S_2 \rightarrow S_o$ emission, but the spectra measured using λ_{ex} = 325 nm correspond to $S_1 \rightarrow S_o$ emission. For QCT, the quantum yields measured in the CH_3OH-H_2O and CH_3CN-H_2O solvents are roughly the same within experimental errors regardless of the excitation light used. However, for API, the quantum yields measured in the CH_3CN-H_2O mixed solvents are larger than those in the CH_3OH-H_2O mixed solvents. This change of quantum yield of API according to different solvent systems is very large if λ_{ex} is 325 nm. The change of quantum yields as a function of water concentration in the various CH_3OH-H_2O and CH_3CN-H_2O mixed solvents for QCT and API is consistent with the strength of the intermolecular hydrogen bonding interaction between the solutes and H_2O according to the increased water content of the solvents. The lifetime change of QCT and API as a function of water composition roughly follows the same pattern as the change of the quantum yield in both CH_3OH-H_2O and CH_3CN-H_2O mixed solvents. The lifetimes of QCT and API in CH_3CN-H_2O are longer than those in CH_3OH-H_2O, but this difference in API is much larger than that of QCT. The decreasing API lifetime due to the increased water content in CH_3OH-H_2O occurs much more quickly than that in CH_3CN-H_2O. These experimental results well support the previously explained ESICT and ESIPT, and characteristic fluorescence properties of QCT and API.

To more closely examine the influence of the bulk dielectric effects and specific hydrogen bonding interactions on the radiative and nonradiative deactivation process, ln(k_{nr}) and ln(k_r) were plotted as a function of the solvatochromic parameters of the mixed solvents as shown in Figures 8 and 9. In the CH_3OH-H_2O mixed solvents, as the π^* or α value increases, the ln(k_{nr}) of QCT increases approximately linearly, but the ln(k_{nr}) of API grows more and more quickly as shown in Figures 8(a) and (b). The shapes of ln(k_{nr}) *vs* π^* plot and ln(k_{nr}) *vs* α plot of QCT and API are similar in the CH_3CN-H_2O solvents as shown in Figures 8(c) and (d). The ln(k_{nr}) of QCT and API increases nearly linearly due to the increase of π^* value and ln(k_{nr}) of both molecules increases slowly at first due to the increasing α value, but this value grows very rapidly at large α values in CH_3CN-H_2O. As such, the change of k_{nr} of QCT and API as a function of π^* or α is different in the CH_3OH-H_2O mixed solvent, but this change of QCT and API is similar in CH_3CN-H_2O mixed solvents. The ln(k_r) value was plotted as a function of π^* or α as shown in Figure 9. In both CH_3OH-H_2O and CH_3CN-H_2O, the shapes of the ln(k_r) *vs* π^* and ln(k_r) *vs* α plot of QCT and API are much different compared with the change of ln(k_{nr}) as a function of the solvent parameters, especially in CH_3CN-H_2O. These plots also differ significantly depending on whether the CH_3OH-H_2O or CH_3CN-H_2O mixed solvent is used. Moreover, the k_r values of API are more sensitive to the change of solvatochromic parameters compared with those of QCT in the CH_3OH-H_2O and CH_3CN-H_2O solvents. In CH_3OH-H_2O, ln(k_r) of QCT decreases slowly but ln(k_r) of API decreases quickly and turns to increases at the end of the plot as the π^* or α value increases. In CH_3CN-H_2O, the ln(k_r) of QCT increases slowly whereas the ln(k_r) of API decreases quickly due to the increased solvent π^* values. In the ln(k_r) *vs* α plot in CH_3CN-H_2O, the k_r value of QCT and API initially remains roughly constant, but the k_r of QCT starts to increase slightly, and the k_r of API begins to decrease quickly and greatly as the amount of

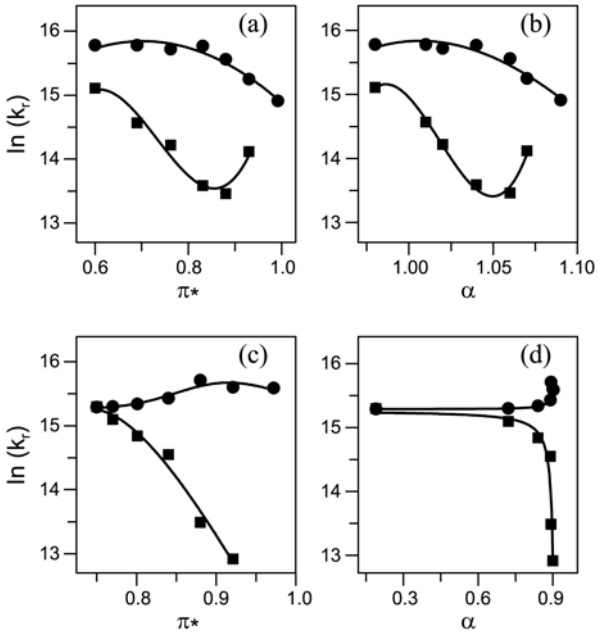

Figure 9. Logarithm of the radiative rate constants (k_r) plotted as a function of the solvent polarity parameter (π^*) or hydrogen-bond donating strength (α) in CH_3OH-H_2O (a, b) and CH_3CN-H_2O (c, d) solvent mixtures; quercetin (●) and apigenin (■). The solid lines are the best polynomial regression fits to the data.

water approaches 20% in solvents. Except for the ln(k_{nr}) *vs* π^* plots and ln(k_{nr}) *vs* α plots in CH_3CN-H_2O, the k_{nr} and k_r values of API are more sensitive to changes in the solvatochromic parameters compared with those of QCT. Finally, the effect of solvent on the excited state dynamics of QCT and API is significantly different according to the solvent system used. This difference will be caused mainly by the microheterogeneity and preferential salvation of CH_3CN-H_2O mixed solvent because H_2O and CH_3OH are protic, whereas CH_3CN is an aprotic solvent. Therefore, the radiative and nonradiative deactivation process of QCT and API will obviously be influenced by both the bulk dielectric effect and the specific hydrogen-bonding interaction of the solvents.

Conclusions

Although QCT and API have been known as nonfluorescent compounds, anomalous characteristic fluorescence properties of these molecules have been discovered in various hydro-organic mixed solvents. For QCT, because of the hydrogen bond-like interaction between the proton on the 2' or 6' of the B ring and the 3-OH moiety, the dihedral angle of the B ring with the rest of molecule is close to 0° and the optimized molecular structure is completely planar in the gas phase. However, for the API, the B ring is slightly twisted relative to the plane of γ-pyrone ring at about 17° due to absence of the 3-OH group at the ground state. However, API becomes almost planar at the S_1 state because the dihedral angle decreases to 2.8°.

In aqueous solution, since the intermolecular hydrogen bond between the polar groups of solute and H_2O will surpass the various intramolecular hydrogen bonds, the dihedral angle will be large, making it very difficult for ESICT to occur. Because the radiationless pathway by way of the formation of a distorted excited state will become very active in water, no fluorescence emission is observed. In CH_3OH and CH_3CN, almost all of the QCT and API molecules have several intramolecular hydrogen bonds between the -OH group and carbonyl oxygen. In this case, since the ESICT should occur easily, QCT and API can exhibit fluorescence emission. Also, another excited state phenomenon, ESIPT, can occur between the 5-OH and keto oxygen *via* an intramolecular hydrogen bond. The "nodal plane" model demonstrates that the S_1 state is much more susceptible to ESIPT compared with the S_2 state. ESIPT can occur quickly in QCT due to the plane molecular structure. Since the formation of the distorted excited state by this ESIPT could be the result of interactions between the emitting state and other nearby excited states, the $S_1 \rightarrow S_o$ fluorescence emission of QCT have not been observed in the organic solvents. For API, ESIPT at the S_1 state cannot occur rapidly because the first relaxation process after pumping occurs through molecular planarization. Because the API at the S_1 state can produce the fluorescence emission from an excited state structure that has not yet undergone the ESIPT process, API exhibits the $S_1 \rightarrow S_o$ emission in the organic solvents. When the QCT and API are excited to the S_2 state, it will be very difficult to take place ESIPT, but on the other hand ESICT should occur easily. Because the FC factors of QCT and API involved in the $S_2 \rightarrow S_1$ internal conversion will be very small, QCT and API exhibit strong $S_2 \rightarrow S_o$ fluorescence emission in the organic solvents. If the molecules are excited to the S_1 state, QCT exhibits no emission but API shows significant fluorescence emission. As the QCT and API are excited to the S_2 state, both molecules show $S_2 \rightarrow S_o$ emission only. Therefore, the major reason why QCT and API exhibit such different characteristic fluorescence properties may be caused by the difference of the dihedral angle of the B ring with the rest of molecules being between QCT and API in the ground state. This suggestion was further supported by the theoretical treatments in which the changes of the molecular orbital and the potential energy surfaces due to excitation were calculated.

The fluorescence properties were measured using different excitation wavelength. The quantum yields of QCT and API decrease gradually in the CH_3OH-H_2O and CH_3CN-H_2O mixed solvents as the solvent water content increases. The fluorescence lifetime change of QCT and API as a function of water composition in both CH_3OH-H_2O and CH_3CN-H_2O solvents demonstrates roughly the same pattern as the change of the quantum yields. The changes of k_r and k_{nr} as a function of π^* or α in CH_3OH-H_2O and CH_3CN-H_2O differ from each other. In the CH_3OH-H_2O mixed solvents, the change of k_{nr} of QCT and API as a function of π^* or α is somewhat different, whereas in the CH_3CN-H_2O mixed solvents, these QCT and API plots are similar to each other. The ln(k_r) *vs* π^* and ln(k_r) *vs* α plot of QCT and API are different in CH_3OH-H_2O mixed solvents but these plot of

QCT and API are much more different in CH_3CN-H_2O mixed solvents. Therefore, the k_r and k_{nr} values of QCT and API will be affected by both the bulk dielectric effect and the specific hydrogen-bonding interaction of the hydro-organic mixed solvents. Eventually, the characteristic fluorescence properties of QCT and API were explained using the ESICT and ESIPT. Because use of the hydro-organic mixed solvents is especially suitable for emulating biological conditions, these kinds of studies will provide valuable information that should help us understand the mechanisms of various strong biological activities of QCT and API.

Acknowledgments. This research was supported by the Basic Science Research Program through the National Research Foundation of Korea funded by the Ministry of Education, Science and Technology (2012-0007862).

References

1. Middleton, E., Jr.; Kandaswami, C. *The Impact of Plant Flavonoids on Mammalian Biology*; Harborne, J. B., Ed.; Chapman and Hall: London, UK, 1994; p 619.
2. Iwashina, T. *J. Plant Res.* **2000**, *113*, 287.
3. Butkoviæ, V.; Klasinc, V.; Bors, W. *J. Agric. Food Chem.* **2004**, *52*, 2816.
4. Exarchou, V.; Nenadis, N.; Tsimidou, M.; Gerothanassis, I. P.; Troganis, A.; Boskou, D. *J. Agric. Food Chem.* **2002**, *50*, 5294.
5. Miyake, Y.; Yamamoto, K.; Morimitsu, Y.; Osawa, T. *J. Agric. Food. Chem.* **1997**, *45*, 4619.
6. Jovanovic, S. V.; Steenken, S.; Tosic, M.; Marjanovic, B.; Simic, M. G. *J. Am. Chem. Soc.* **1994**, *116*, 4846.
7. Lapouge, C.; Dangleterre, L.; Cornard, J. P. *J. Phys. Chem.* **2006**, *110*, 12494.
8. Li, Y. Q.; Zhou, F. C.; Gao, F.; Bian, J. S.; Shan, F. *J. Agric. Food Chem.* **2009**, *57*, 11463.
9. Liu, W.; Rong, G. *J. Coll. Interf. Sci.* **2006**, *302*, 625.
10. Cornard, J. P.; Merlin, J. C. *J. Inorg. Biochem.* **2002**, *92*, 19.
11. Baranac, J. M.; Petranović, N. A.; Dimitrić-Marković, M. D. J. M. *J. Agric. Food Chem.* **1997**, *45*, 1694.
12. Gutierrez, A. C.; Gehlen, M. H. *Spectrochim. Acta A* **2002**, *58*, 83.
13. Rossi, M.; Rickles, L. F.; Halpin, W. A. *Bioorgan. Chem.* **1986**, *14*, 55.
14. Leopoldini, M.; Marino, T.; Russo, N.; Toscano, M. *Theor. Chem. Acc.* **2004**, *111*, 210.
15. Falkovskaia, E.; Sengupta, P. K.; Kasha, M. *Chem. Phys. Lett.* **1998**, *297*, 109.
16. Sengupta, P. K.; Kasha, M. *Chem. Phys. Lett.* **1979**, *68*, 382.
17. Smith, G. J.; Markham, K. R. *J. Photochem. Photobiol. A* **1998**, *118*, 99.
18. Hollman, P. C. H.; van Trijp, J. M. P.; Buysman, M. N. C. P. *Anal. Chem.* **1996**, *68*, 3511.
19. Liu, H. B.; Daun, Y.; Shin, S. C.; Park, H. R.; Park, J. K.; Bark, K. M. *Photochem. Photobiol.* **2009**, *85*, 934.
20. Park, H. R.; Liu, H. B.; Shin, S. C.; Park, J. K.; Bark, K. M. *Bull. Korean Chem. Soc.* **2011**, *32*, 981.
21. Navarro-Nunez, L.; Lozano, M. L.; Palomo, M.; Martinez, C.; Vicente, V.; Castillo, J.; Benavente-Garcia, O.; Diaz-Ricart, M.; Escolar, G.; Rivera, J. *J. Agric. Food Chem.* **2008**, *56*, 2970.
22. Yuan, J. L.; Liu, H.; Kang, X.; Lv, Z.; Zou, G. L. *J. Mole. Struct.* **2008**, *891*, 333.
23. Yuan, J. L.; Iv, Z.; Liu, Z. G.; Hu, Z.; Zou, G. L. *J. Photochem. Photobiol. A* **2007**, *191*, 104.
24. Reichardt, C. *Solvents and Solvent Effects in Organic Chemistry*; VCH, Weinheim, Germany, 1988; p 372.
25. Eaton, D. F. *Reference Compounds for Fluorescence Measurement*; IUPAC Organic Chemistry Division, Washington DC, USA. 1987; p 1.
26. Frish, M. J.; Trucks, G. W.; Head-Gordon, M. H.; Gill, P. M. W.; Wong, M. W.; Foresman, J. B.; Johnson, B. G.; Schlegel, H. B.; Robb, M. A.; Replogle, E. S.; Gomperts, R.; Andres, J. L.; Raghavachari, K.; Binkley, J. S.; Gonzalez, C. R. L.; Fox, D. J.; Defrees, D. J.; Baker, J.; Stewart, J. J. P.; Pople, J. A. *Gaussian 03*; Gaussian Inc., Pittsburgh, PA, USA. 2003.
27. Zsila, F.; Bikádi, Z.; Simonyi, M. *Biochem. Pharmacol.* **2003**, *65*, 447.
28. Favaro, G.; Clementi, C.; Romani, A.; Vickackaite, V. *J. Fluoresc.* **2007**, *17*, 707.
29. Hochstrasser, R. M.; Marzzacco, C. *J. Chem. Phys.* **1968**, *49*, 971.
30. Cornard, J. P.; Boudet, A. C.; Merlin, J. C. *J. Mol. Struct.* **1999**, *508*, 37.
31. Cornard, J. P.; Merlin, J. C.; Boudet, A. C.; Vrielynck, L. *Biospect.* **1997**, *3*, 183.
32. Mendoza-Wilson, A. M.; Glossman-Mitnik, D. *J. Mol. Struct. (Theochem)* **2004**, *681*, 71.
33. Saskia, A. B.; van Acker, E.; de Groot, M. J.; van den Berg, D. J.; Tromp, M. N. J. L.; den Kelder, G. D. O.; van der Vijgh, W. J. F.; Bast, A. *Chem. Res. Toxicol.* **1996**, *9*, 1305.
34. Cody, V.; Luft, J. R. *J. Mol. Struct.* **1994**, *317*, 89.
35. Amat, A.; Clementi, C.; De Angelis, F.; Sgamellotti, A.; Fantacci, S. *J. Phys. Chem. A* **2009**, *113*, 15118.
36. Matías Funes, N.; Correa, M.; Silber, J. J.; Biasutti, M. A. *Photochem. Photobiol.* **2007**, *83*, 486.
37. Martinez, M. L.; Studer, S. L.; Chou, P. T. *J. Am. Chem. Soc.* **1991**, *113*, 5881.